EFFECT OF HEAT TREATMENT ON SOME MECHANICAL PROPERTIES OF Ni-Al-Cr TYPE INTERMETALLIC ALLOY MODIFIED WITH ADDITIONS OF Ta, Mo AND Zr

MILAN FLORIAN[1]

The effect of heat treatment on room temperature microhardness, hardness and tensile properties of directionally solidified and heat-treated multiphase intermetallic alloy with chemical composition Ni-10.65Al-6.79Cr-4.90Ta-2.44Mo-0.96Zr-0.078Fe [wt.%] was studied. Except of γ, γ', α, and β phases the alloy contained eutectic regions with Zr-rich phase. The chemical composition of Zr-rich phase was determined as Ni-4.9Al-8Cr-5Mo--1.9Ta-19.1Zr [wt.%]. The volume fraction of eutectic regions decreased with increasing time of annealing. The melting temperature of the eutectic was measured to be 1453 K. Annealing at 1493 K and gas fan cooling to room temperature caused a decrease of microhardness of interdendritic region and significant increase of microhardness of dendrites. Consecutive ageing at 1173 K caused a decrease of hardness and microhardness. During the first stages of ageing the ultimate tensile strength rapidly decreased, but after 4800 s of ageing, increased. Generally, heat treatment caused significant embrittlement of the alloy.

K e y w o r d s: Ni-based intermetallics, mechanical properties, directional solidification

VPLYV TEPELNÉHO SPRACOVANIA NA NIEKTORÉ MECHANICKÉ VLASTNOSTI INTERMETALICKEJ ZLIATINY TYPU Ni-Al-Cr MODIFIKOVANEJ Ta, Mo A Zr

V práci sme študovali vplyv tepelného spracovania na tvrdosť, mikrotvrdosť a ťahové vlastnosti pri izbovej teplote usmernene kryštalizovanej a tepelne spracovanej multifázovej intermetalickej zliatiny s chemickým zložením Ni-10,65Al-6,79Cr-4,90Ta-2,44Mo-0,96Zr--0,078Fe [hm.%]. Okrem fáz γ, γ', α a β obsahovala zliatina aj eutektické oblasti s fázou bohatou na Zr. Chemické zloženie fázy bohatej na Zr bolo Ni-4,9Al-8Cr-5Mo-1,9Ta-19,1Zr [hm.%]. Objemový podiel eutektika sa znižoval so zvyšujúcim sa časom žíhania. Stanovili sme teplotu tavenia eutektika na 1453 K. Žíhanie pri 1493 K následným ochladením na izbovú teplotu v prúde stlačeného vzduchu spôsobilo zníženie mikrotvrdosti medzidendritického priestoru a výrazné zvýšenie mikrotvrdosti dendritov. Následné starnutie pri

[1] Institute of Materials and Machine Mechanics of the SAS, Račianska 75, 831 02 Bratislava 3, Slovak Republic, e-mail: ummslapi@savba.sk

1173 K spôsobilo zníženie tvrdosti a mikrotvrdosti. Rozpúšťacie žíhanie spôsobovalo zvýšenie mikrotvrdosti dendritov a medzidendritického priestoru. Starnutie spôsobovalo pokles tvrdosti a mikrotvrdosti. Medza pevnosti v ťahu v prvých štádiách starnutia výrazne klesala, ale po 4800 s sa začala zvyšovať. Vo všeobecnosti tepelné spracovanie spôsobilo výrazné skrehnutie zliatiny.

1. Introduction

Mechanical properties of Ni_3Al single phase are insufficient for most high-temperature structural applications. However, mechanical properties of Ni_3Al can be significantly improved by modification of microstructure through an appropriate alloying and processing techniques. It has been found that alloying by various elements such as B, Cr, Mo, Zr etc., from the group IVB-VIIIB of the periodic table improved room-temperature ductility and reduced brittleness at higher temperatures (above 873 K) in single phase alloys [1–3]. Further increase of mechanical properties can be achieved by a higher content of alloying elements that results in formation of multiphase structures. The multiphase Ni_3Al-based intermetallic alloys for structural applications have been intensively studied around the world in the last decade. These alloys are attractive because of their high strength at all temperatures and acceptable ductility at room temperature. It has been shown that additions of chromium from 5 to 21 at.% and other elements (Co, Fe, Ti, Mo, Zr, B) to binary Ni_3Al result in multiphase microstructures composed of ordered Ni_3Al (γ'-phase), NiAl (β-phase), γ-phase (Ni-based solid solution), α-Cr (Cr-based solid solution) precipitates [4] and complex compounds with zirconium [5]. Several types of multiphase nickel-based intermetallic alloys such as γ/γ'-α, γ/γ'-β and β-γ'-γ-α were intensively studied in details during recent several years [6–12]. However, limited work has been performed on directionally solidified (DS) Ni_3Al-based multiphase intermetallic alloys and studies of mechanical properties of such materials are still lacking in the literature [12–16]. Therefore, new investigations of microstructure and mechanical behaviour of DS Ni_3Al-based multiphase alloys for high temperature applications are of great fundamental and applied research interest.

The aim of the present paper is to extend the previous studies on DS Ni-Al-Cr type intermetallic alloys modified by iron and titanium [12–16]. This paper aims at the evaluation of the effect of high temperature solid solution annealing and intermediate temperature ageing on the microstructure and mechanical properties of DS Ni-Al-Cr type intermetallic alloy modified with additions of tantalum, molybdenum and zirconium.

2. Experiment

Master ingots with chemical composition given in Table 1 were prepared in vacuum induction furnace by melting of high purity metals under an argon atmo-

Table 1. Chemical composition of Ni_3Al-based multiphase alloy [wt.%]

Ni	Al	Cr	Ta	Mo	Zr	Fe
Balance	10.65	6.79	4.90	2.44	0.96	0.078

sphere using an exo-melt process and casting into graphic moulds [18]. These ingots were machined into rods and placed in high-purity alumina crucibles with outside diameter of 15 mm and wall thickness of 2 mm. Ingots for ageing and mechanical tests were prepared by directional solidification in a modified Bridgman-type apparatus at a constant growth rate of $V = 5.56 \times 10^{-5}$ m·s^{-1} and constant temperature gradient in the melt at solid-interface of $G_L = 15 \times 10^3$ K·m^{-1}. The basic apparatus arrangement with an analysis of directional solidification process can be found elsewhere [19].

Phase transformations of the alloy were determined by differential thermal analysis (DTA) performed in a NETZSCH apparatus at heating and cooling rates of 8.33×10^{-2} K·s^{-1} under argon atmosphere.

Heat treatments were proceeded in a NABERTHERM resistance furnace in following steps: (1) high temperature solid solution annealing at 1493 K for 14400 s followed by a gas fan cooling to room temperature and (2) ageing at intermediate temperature of 1173 K for a time varying from 0 to 43200 s followed by a gas fan cooling to room temperature. All heat treatments were performed in air.

Hardness measurements were performed by a Vickers' method using device HECKERT HPO 250 at a load of 294.2 N during 10 s. Microhardness was measured by standard Vickers method at a load of 0.066 N during 10 s. Room temperature tensile tests were conducted on flat tensile specimens with a gauge length of 50 mm, width of 5 mm and thickness of 4 mm at an initial strain rate of 3.33×10^{-4} s^{-1} using a screw-driven INSTRON machine.

Microstructural analysis was performed by optical microscopy, scanning electron microscopy (SEM) and energy-dispersive spectroscopy (EDS). Samples for optical microscopy and SEM were prepared using standard metallographic techniques and chemically etched in a solution of 150 ml H_2O, 25 ml HNO_3 and 10 ml HF. SEM investigations were performed by JEOL JSM-5310 microscope equipped by energy-dispersive spectrometer KEVEX. Quantitative analyses were performed by computerised image analyser.

3. Results and discussion

3.1 Microstructure

Directionally solidified ingots consisted of columnar grains (3-6) elongated parallel to the ingot axis. The microstructure within columnar grains consisted of dendrites with well-developed tertiary arms and interdendritic region. The volume fraction of dendrites after directional solidification was measured to be about 38

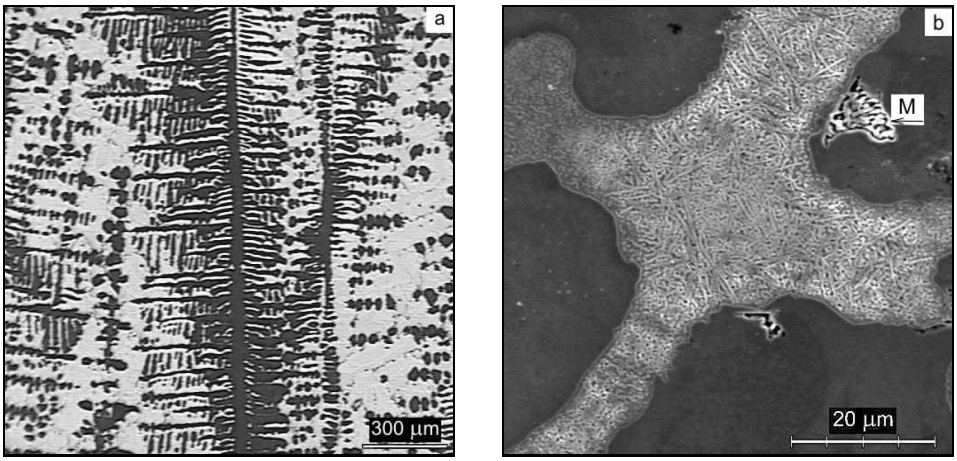

Fig. 1. Microstructure of DS multiphase Ni-based intermetallic alloy: a) optical micrograph of longitudinal section with typical dendritic morphology; b) SEM micrograph showing microstructure of interdendritic region, dendrite and region M.

vol.% and primary dendrite arm spacing was determined to be 2.27×10^{-5} m. Figure 1a shows morphology of dendrites on a longitudinal section of DS ingot. Figure 1b illustrates the dendrite morphology on a transverse section. As shown by Lapin et al. [12] for an alloy with similar chemical composition, the dendrite consists of β-matrix (intermetallic NiAl phase), coarse γ'-particles (intermetallic Ni_3Al phase), fine γ'-needles, and spherical α-precipitates (Cr-based solid solution). The interdendritic regions contain ordered domains of γ'-phase surrounded by γ-matrix (Ni-based solid solution). However, the present alloy contains in addition new regions (M) formed at the dendritic-interdendritic interfaces, as shown in Fig. 1b. It should be noted that such regions were not observed in quaternary Ni-Al-Cr-Ti systems by previous authors [12].

Figure 2 shows the DTA heating and cooling curves of the studied intermetallic alloy. From this figure, the solidus and liquidus temperature were determined to be 1597 and 1654 K, respectively. In addition, there is an evidence of an endothermic reaction at 1453 K. Microstructural observation of DTA samples revealed that this endothermic reaction corresponds to further formation of regions (M).

Table 2 summarises the chemical composition of Zr-rich phase, interdendritic region and dendrites. As seen from this table, the region is enriched by zirconium. The content of Zr in this region is about 19-times higher than its original average content in the master alloy. The contents of other elements like Ni, Al and Ta are lower and Cr and Mo are higher than in the master alloy. Since there is no available phase diagram or phase composition of alloy with a similar chemical composition

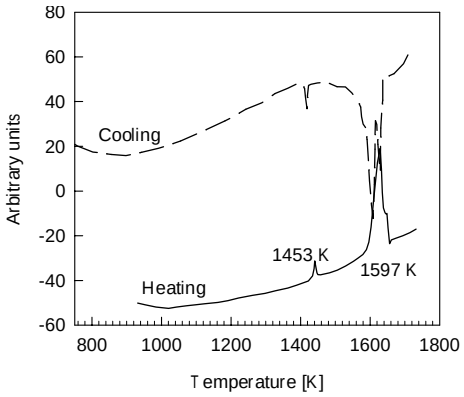

Fig. 2. DTA of multiphase intermetallic alloy.

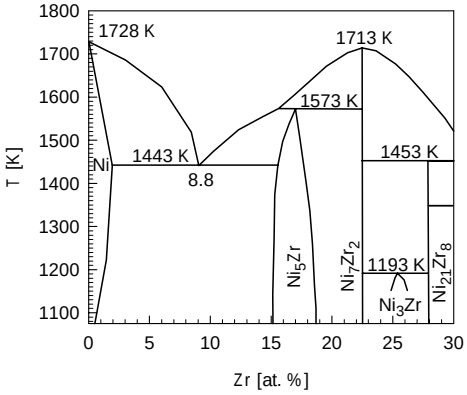

Fig. 3. Scheme of binary Ni-Zr phase diagram from Ni-rich corner.

Table 2. EDS analysis of dendrites, interdendritic region and Zr-rich phase [wt.%]

	Ni	Al	Cr	Mo	Ta	Zr
Dendrite	71.01	16.83	8.12	0.66	3.15	0.22
Interdendritic region	77.35	8.52	5.95	1.04	6.09	1.05
Zr-rich phase	61.1	4.9	8.0	5.0	1.9	19.1

in the literature, a binary phase diagram was used as a first approximation to determine coexisting phases in such multiphase region. Figure 3 illustrates the part of Ni-Zr binary phase diagram used for this purpose. Assuming the chemical composition of Zr-rich phase given in Table 2 and binary phase diagram in Fig. 3, the Zr-rich phase can be considered to belong to an intermetallic compound Ni_5Zr. In addition, the determined endothermic reaction at 1453 K corresponds very well to the eutectic phase transformation at 1443 K in the binary Ni-Zr phase diagram.

Lee et al. [5] tried to determine the type of Zr-rich phase in Ni_3Al-based intermetallic alloy with addition of 0.93 wt.% of Zr. They found out that the chemical composition of the phase was 70.79Ni-6.75Al-22.46Zr [wt.%]. Analysis of their electron diffraction patterns revealed that this phase contained ordered FCC crystal structure with lattice parameter of 6.9×10^{-10} m. However, the authors were not able to determine the zirconium rich phase exactly. Li and Chaki [21] showed similar phase in Ni_3Al-based intermetallic alloys IC-50 and IC-218 alloyed with various content of Zr ranging from 0.6 to 0.86 wt.%. The chemical composition of their zirconium-rich phase was close to Ni_7Zr_2, but they did not succeed in exact determining of this phase.

In spite of the fact that TEM studies are not the subject of the present work, it should be noted that our preliminary TEM investigations did not clearly prove Ni_5Zr or Ni_7Zr_2 phases in the studied alloy. This can be explained by the fact that our specimens subjected to TEM analysis were quenched after solid solution annealing which significantly affected the crystal structure of zirconium rich phase.

3.2 Influence of heat treatment on microstructure

Figure 4 represents the microstructure of multiphase intermetallic alloy after

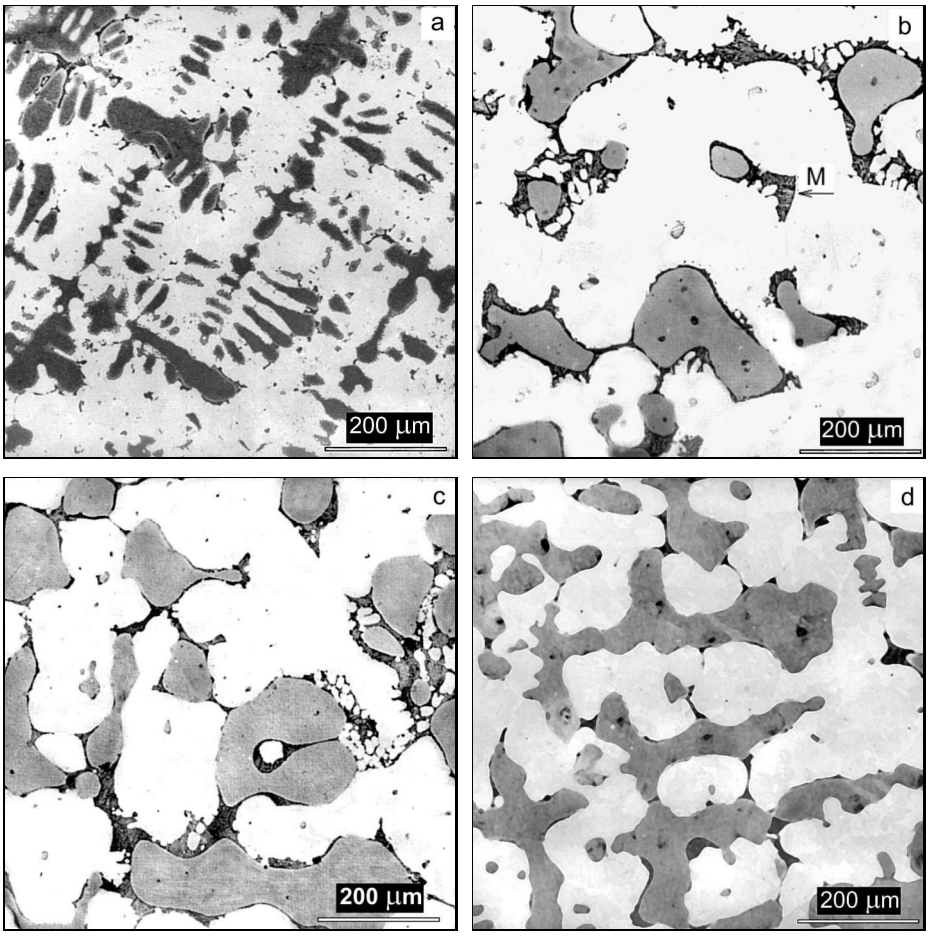

Fig. 4. Optical micrographs of DS Ni-based intermetallic alloy: a) without heat treatment; b) solid solution annealing at 1493 K for 14400 s; c) solid solution annealing at 1493 K for 14400 s followed by ageing at 1173 K for 3600 s; d) solid solution annealing at 1493 K for 14400 s followed by ageing at 1173 K for 43200 s.

various heat treatments. During annealing at 1493 K for 14400 s the α and γ' precipitates were dissolved in the β-dendrites. Dendritic β-phase coagulated and the discontinuous eutectic regions containing Zr-rich phase changed to continuous layer covering the dendrites. Consecutive ageing at 1173 K for 43200 s resulted in a decrease of the volume fraction of dendrites from 38 to about 29 vol.%.

The time of solid solution annealing at 1493 K affected volume fraction of eutectic regions containing Zr-rich phase. Figure 5 is a plot of the volume fraction V_e of the eutectic regions (M) with Zr-rich phase as a function of annealing time t_a at 1493 K. It is evident that the volume fraction of the eutectic decreased to about 60 % when the time of annealing increased by four times. The volume fraction of the eutectic affects the porosity of the alloy after the heat treatments. During cooling from the solid solution annealing temperature the liquid eutectic solidifies and forms draws and pores at the dendritic-interdendritic interfaces. Taking into account the final porosity of the annealed specimens and their oxidation at 1493 K, the optimal time of the solid solution annealing was found to be 14400 s. This constant annealing time of 14400 s at 1493 K was used for all specimens, which were subjected to evaluation of mechanical properties.

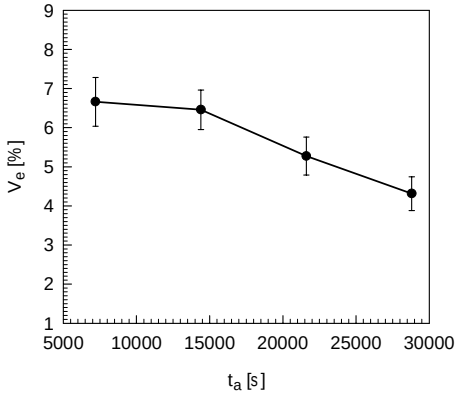

Fig. 5. Time dependence of volume fraction of eutectic with Zr-rich phase during annealing at 1493 K.

3.3 Influence of heat treatment on mechanical properties

Figure 6 shows the evolution of microhardness of dendrites and interdendritic region with the ageing time at 1173 K. The microhardness HV_m of dendrites and interdendritic region after directional solidification were measured to be 581 and 426, respectively. From Fig. 6, it is evident that the microhardness of dendrites and interdendritic region increased after annealing at 1493 K followed by gas fan cooling ($t = 0$). Ageing time up to 9900 s resulted in a rapid decrease of the microhardness of dendrites. During longer ageing time the microhardness increased and reached nearly constant value after ageing for 15900 s. As was proved by Lapin et al. [4, 12] such variation of the microhardness is due to size, shape and distribution of α and γ' precipitates in the β-dendrites and α and γ' precipitates in the interdendritic region. The similar trend showed the evolution of Vickers' hardness, as illustrated in Fig. 7. In this case, the minimum hardness values were reached after ageing for 4800 s. This shift of minimum hardness values to lower ageing time in comparison with the

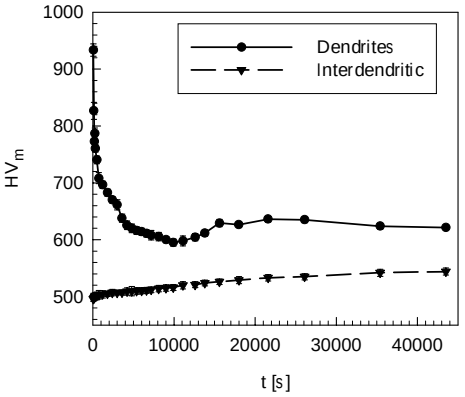

Fig. 6. Time dependence of microhardness of dendrites and interdendritic region during ageing at 1173 K.

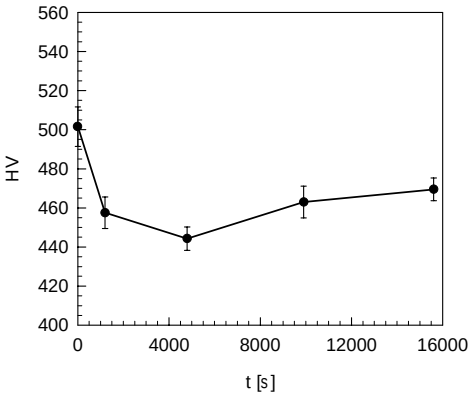

Fig. 7. Time dependence of hardness during ageing.

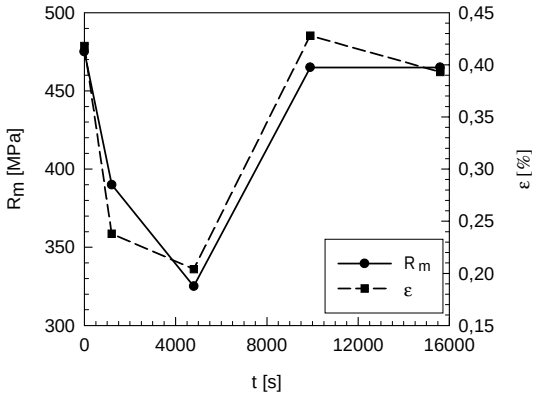

Fig. 8. Time dependence of ultimate tensile strength and elongation.

microhardness was caused by including of the interdendritic region characterised by a significant lower microhardness values to the hardness measurements.

Figure 8 characterises the evolution of ultimate tensile strength and elongation with ageing time at 1173 K. It was not possible to determine the offset yield strength, because of negligible plastic deformation of all samples. The evolution of ultimate tensile strength with annealing time corresponded approximately to the evolution of the Vickers' hardness but no definite relationship could be found between them. The ultimate tensile strength of the samples after directional solidi-

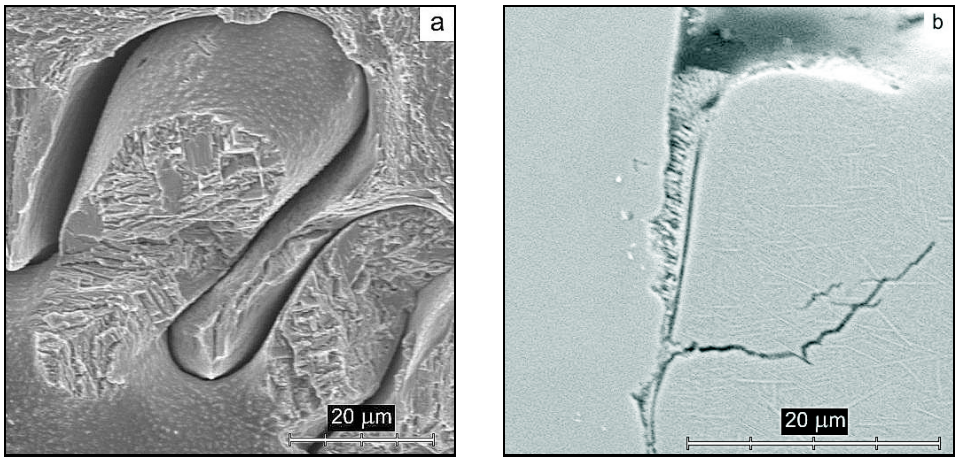

Fig. 9. Fractography of DS multiphase Ni-based intermetallic alloy solid solution annealed at 1493 K for 14400 s and aged at 1173 K for 4800 s: a) decohesion between dendrites and interdendritic region; b) crack propagation from eutectic with Zr-rich phase into the dendrite.

fication was measured to be 783 MPa, the 0.2 % offset yield strength was 585 MPa and tensile elongation was about 2.8 %. It is clear that the applied heat treatment caused great embrittlement of the alloy connected with significantly lower values of the ultimate tensile strength and tensile ductility.

Figure 9 shows the SEM micrograph of fracture surface of tensile specimens. A decohesion was the main mechanism governing the fracture between β-dendrites and interdendritic region. Similar decohesion during room temperature tensile tests was also observed by Lapin et al. [4] in Ni-Al-Cr-Ti type alloy. However, in the case of the present alloy the decohesion was primarily caused by the eutectic layer formed at the dendritic-interdendritic interfaces. The cracks primarily nucleated and propagated along dendritic-

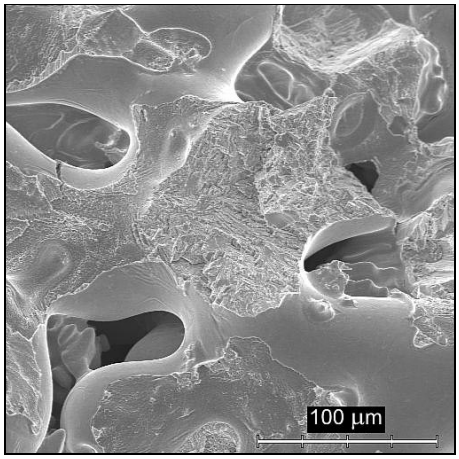

Fig. 10. SEM micrograph of fracture surface of DS multiphase Ni-based intermetallic alloy after solid solution annealing at 1493 K for 14400 s and gas fan cooling to room temperature.

interdendritic boundaries and then propagated through the brittle dendrites. It should be noted that significant effect on the crack initiation and propagation had porosity formed within the eutectic regions. Figure 10 illustrates such large porosity formed around fractured dendrites.

4. Conclusions

The effect of ageing and annealing on microstructure and mechanical properties of DS Ni_3Al-based multiphase intermetallic alloy was studied. The experimental results support the following conclusions:

1. After directional solidification the microstructure of the studied alloy was composed of γ, γ', α, and β phases and eutectic regions containing Zr-rich phase. The chemical composition of Zr-rich phase formed at the dendritic-interdendritic interfaces was determined to be Ni-4.9Al-8Cr-5Mo-1.9Ta-19.1Zr [wt.%]. According to DTA, EDS and binary phase diagram the Zr-rich phase was assumed to belong to Ni_5Zr intermetallic compound.

2. The amount of eutectic region containing Zr-rich phase decreased with increasing solid solution annealing time. The melting temperature of the eutectic region was determined to be 1493 K. During solid solution annealing and cooling the porosity is formed within the eutectic region.

3. Solid solution annealing at 1493 K and gas fan cooling of specimens caused a decrease of microhardness of interdendritic region and significant increase of microhardness of dendrites. Consecutive ageing at 1173 K caused a decrease of hardness and microhardness of the alloy. The ultimate tensile strength of heat-treated specimens decreased with increasing the ageing time up to 4800 s and increased at longer ageing time. Heat treatment caused large embrittlement of the alloy connected with significantly lower values of the ultimate tensile strength and tensile ductility in comparison with DS specimens.

4. During tensile testing the fracture of the specimen is caused by decohesion at the dendritic-interdendritic interfaces and by nucleation and propagation of cracks within the eutectic regions and brittle dendrites.

Acknowledgements

The author gratefully acknowledges the financial support of the Slovak Grant Agency for Science under the contract VEGA 2/1044/21.

REFERENCES

[1] PRETORIUS, T.—BAITHER, D—NEMBACH, E.: Acta Mater., *49*, 2001, p. 1981.
[2] CZEPPE, T.—WIERZBINSKI, S.: Inter. J. Mech. Sci., *42*, 2000, p. 1499.
[3] FLORIAN, M.: Kovove Mater., *38*, 2000, p. 5.
[4] LAPIN, J.: Intermetallics, *5*, 1997, p. 615.
[5] LEE, J. H.—CHOE, B. H.—LEE, Z. H.: Scripta Mater., *40*, 1999, p. 853.

[6] LAPIN, J.: Kovove Mater., *35*, 1997, p. 43.
[7] WHITTENBERGER, J. D.—RAJ, S. V.—LOCCI, I. E.—SALEM, J. A.: Intermetallics, *7*, 1999, p. 1159.
[8] LAPIN, J.—IVAN, J.: Scripta Metall. Mater., *33*, 1995, p. 391.
[9] GALE, W. F.—ABDO, Z. A. M.—NEMANI, R. V.: J. Mater. Sci., *34*, 1999, p. 407.
[10] LAPIN, J.—DELANNAY, F.: Metall. Mater. Trans. A, *26A*, 1995, p. 2053.
[11] CHEN, R. S.—GUO, J. T.—YIN, W. M.—ZHOU, J. I.: Scripta Mater., *40*, 1998, p. 209.
[12] LAPIN, J.—PELACHOVÁ, T.—BAJANA, O.: Intermetallics, *8*, 2000, p. 1417.
[13] LAPIN, J.—KLIMOVÁ, A.—VELÍSEK, R.—KURSA, M.: Scripta Mater., *37*, 1997, p. 85.
[14] LAPIN, J.: Intermetallics, *7*, 1999, p. 599.
[15] WIERZBINSKI, S.—LAPIN, J.—CZEPPE, T.: Archives of Metallurgy, *44*, 1999, p. 221.
[16] LAPIN, J.—WIERZBINSKI, S.—PELACHOVA, T.: Intermetallics, *7*, 1999, p. 705.
[17] LAPIN, J.: Kovove Mater., 40, 2002, p. 209.
[18] LAPIN, J.: J. Mater. Sci. Technol., *117*, 2001, (No. 3 – Special Issue, CD).
[19] LAPIN, J.: Kovove Mater., *34*, 1996, p. 265.
[20] LAPIN, J.—ONDRÚŠ, Ľ.: Kovove Mater., *40*, 2002, p 161.
[21] LI, H.—CHAKI, T. K.: Mater. Sci. Eng. A, *A192/193*, 1995, p. 570.

Received: 30.4.2002